Vertically integrated optics for ballistic electron emission luminescence: Device and microscopy characterizations

Wei Yi,[a] Ian Appelbaum,[b] Kasey J. Russell, and Venkatesh Narayanamurti
Gordon McKay Laboratory of Applied Science, Harvard University, Cambridge, Massachusetts 02138

Richard Schalek
Center for Nanoscale Systems, Harvard University, Cambridge, Massachusetts 02138

Micah P. Hanson and Arthur C. Gossard
Materials Department, University of California, Santa Barbara, California 93106

(Received 8 December 2005; accepted 17 April 2006; published online 6 July 2006)

By integrating a *p-i-n* photodiode photodetector directly into a ballistic electron emission luminescence (BEEL) heterostructure with GaAs quantum-well active region, we have obtained a photon detection efficiency of more than 10%. This is many orders of magnitude higher than conventional far-field detection scheme with the most sensitive single-photon counters, enabling BEEL microscopy in systems with no optical components. Detailed analysis shows found a parasitic bipolar injection in parallel with the desired optical coupling between the BEEL heterostructure and the integrated photodiode beyond a characteristic collector bias, which may be solved by improved device design or limiting the operating window of the collector bias. Preliminary BEEL microscopy images of a homogeneous GaAs quantum-well luminescent layer show lateral variations of photon emission correlated with the collector current injection level modulated by surface features or interface defects. © *2006 American Institute of Physics*. [DOI: 10.1063/1.2208738]

I. INTRODUCTION

As a recent development of ballistic electron emission microscopy/spectroscopy (BEEM/BEES),[1,2] ballistic electron emission luminescence (BEEL) utilizes a voltage-biased direct-gap semiconductor bipolar heterostructure to collect hot electrons ballistically injected by a tunnel junction over a Schottky barrier, where these hot electrons may radiatively recombine with holes and emit interband luminescence given enough collector bias.[3] The energy and polarization of emitted photons can be probed to determine the quantum-confined electronic states in the active region. Combining BEEL with collector current spectroscopy (BEES), which is a sensitive probe of the buried potential profiles, a simultaneous electronic and photonic characterization of semiconductor heterostructures is possible. If the tunnel emitter is a scanning tunneling microscope (STM) tip,[4,5] it is possible to acquire a laterally resolved luminescence map of active layers buried beneath the metal-semiconductor interface, together with concurrent imaging of surface topography (STM) and interface electron transmission (BEEM). Such a technique would be a valuable characterization tool to study *local* carrier transport and spontaneous emission properties for optoelectronic devices based on nanoscaled materials such as self-assembled quantum dots[6–8] and nanocrystals.[9]

However, BEEL operation in STM mode is very challenging. To obtain the spatial resolution, a sharp tip with very small effective tunnel-junction area ($\sim 10\ \mathrm{nm}^2$) must be used, correspondingly the maximum tunnel current is in the order of 10^0-10^1 nA. After the attenuation in the metal base, quantum mechanical reflection at the metal-semiconductor interface, hot-electron current finally injected into the semiconductor collector is only 10^0-10^2 pA. Moreover, not all the injected electrons are able to radiatively recombine with holes. Device simulations[10] indicate that nonradiative recombination through deep levels may become a dominant mechanism for such low minority injection levels. This adds stringent requirements on device design, choice of materials, and crystal growth. Despite these difficulties, BEEL from GaAs quantum well[3,4] (QW) and InAs quantum dots[5] has been successfully demonstrated using far-field detection methods, albeit the small signal level in STM mode was not enough to perform a spectrometer analysis.

Because photon detection may become a bottleneck for BEEL microscopy, emphasis must be given to improving the detection efficiency. For the conventional far-field light collection scheme, considering the efficiency of light out coupling for dielectric materials, the detected photons are only a small fraction of the total emitted photons. This scheme may not give sufficient signal-to-noise ratio, especially for structures with relatively low internal quantum efficiencies. There are also other disadvantages such as alignment requirements and the issue of integration with a cryogenic STM system. Since photons detected will eventually be converted to electric signals by an optoelectronic transducer, any optical element used to transmit these photons from the light source to the photodetector will increase the loss. Therefore, photon detection would be optimized if the optical elements were eliminated entirely and the detector is placed to the closest possible distance to the light source. Taking advantage of epitaxial growth technologies or wafer transfer methods, it is possible to join a photodetector with matched refractive in-

[a]Electronic mail: wyi@fas.harvard.edu
[b]Present address: Electrical and Computer Engineering Department, University of Delaware, Newark, Delaware 19716.

deces, such as a *p-i-n* photodiode or avalanche photodiode, onto the BEEL heterostructure without affecting the device characteristics. Both light extraction and light collection would be optimized with such an integrated-optics scheme. It is noteworthy that the concept of such an integrated device bears some similarity to the integrated photon upconversion devices combining a quantum-well infrared photodetector (QWIP) and a light-emitting diode (LED) together on the same wafer,[11,12] although they serve very different purposes.

In this article, an alternative to the far-field detection scheme of collecting photons emitted from a BEEL device is proposed and explored. A *p-i-n* photodiode photodetector is directly integrated into the *monolithic* BEEL heterostructure, which may enable measuring luminescence with the highest possible sensitivity.

II. DEVICE DESIGN

The design of the GaAs/$Al_xGa_{1-x}As$ BEEL heterostructure is based on the previously reported BEEL devices.[3,4,13] A slight modification is made by adding thin spacer layers of undoped AlGaAs on either side of the GaAs QW active region, which is intended to reduce donor-acceptor recombination pathways. Beneath the BEEL heterostructure, a 1 μm thick undoped photon-absorption layer is grown between heavily *p*-doped and *n*-doped materials. To absorb the interband emission from the GaAs QW, the absorption edge of the undoped layer is effectively lowered by growing a superlattice (SL) of 20 periods of 40/10 nm GaAs/$In_{0.05}Ga_{0.95}As$. The overall doping profile of such an integrated-optics BEEL device mimics a *n-p-n* heterojunction bipolar transistor (HBT). However, the "normal" bipolar operation of a HBT, i.e., direct minority carrier (electron) injection through the heavily *p*-doped layer into the photodetector, is undesired, since it will also produce a current signal. The photodetector should only be optically coupled to the luminescent layer. To avoid such a problem, an $Al_{0.45}Ga_{0.55}As$ layer is inserted between the BEEL structure and photodetector as a potential barrier for electrons, which also serves as an etch-stop layer to make collector electrical contact.

The heterostructure device was grown via molecular beam epitaxy with the following structure. A heavily doped *n*-type GaAs substrate, GaAs/InGaAs SL photon-absorption layer, and 100 nm *p*-type GaAs layer doped to 5×10^{18} cm^{-3} form the photodetector. Next, 100 nm *p*-type $Al_{0.30}Ga_{0.70}As$ doped to 5×10^{18} cm^{-3}, 25 nm *p*-type $Al_{0.45}Ga_{0.55}As$ etch-stop layer doped to 5×10^{18} cm^{-3}, and 100 nm *p*-type $Al_{0.30}Ga_{0.70}As$ doped to 5×10^{18} cm^{-3} were grown. The thickness and composition of these p^+ layers are designed to prevent direct minority (electron) injection into the photon-absorption region. Above the p^+ region, the BEEL heterostructure is started with a 5 nm undoped $Al_{0.30}Ga_{0.70}As$ spacer, 10 nm undoped GaAs QW, 5 nm undoped $Al_{0.30}Ga_{0.70}As$ spacer, 100 nm *n*-type $Al_{0.30}Ga_{0.70}As$ doped to 2×10^{17} cm^{-3}, and a 20 nm *n*-type GaAs cap layer doped to 2×10^{17} cm^{-3} finish the growth. In all epitaxial growth, Si is used as *n*-type dopant and Be is used as *p*-type dopant. The substrate dopant is Si. The resulted equilibrium band diagram is shown schematically in Fig. 1.

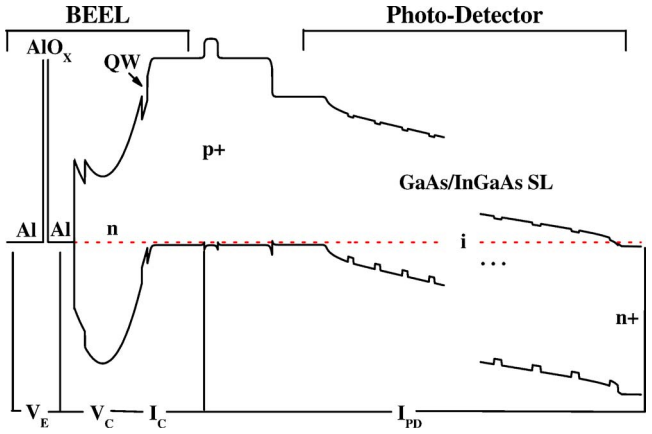

FIG. 1. (Color online) Energy band diagram of a vertically integrated device with BEEL region (left) and integrated photodiode (right), showing emitter bias (V_E), collector bias (V_C), collector current measurement (I_C), and photocurrent measurement (I_{PD}).

III. DEVICE FABRICATION

Previous works have shown that solid-state metal-base transistors help to understand the spectroscopic features of BEEL seen in STM mode[4,5] owing to their much larger collector current level. Therefore, devices terminated with solid-state tunnel junctions were first made to examine the effectiveness of the integrated photodetector. Before the shadow-mask process for fabrication of metal-base transistors, Ohmic contact to the buried p^+ layer (collector) was made by photolithography, wet etching, and subsequent metallization with Cr/Au. To fabricate the Al/AlO_x/Al tunnel junctions, shadow-mask process is used to prevent any contamination to the surface of Al base.[3–5] Masked vacuum deposition of a thin (100 Å) Al base, followed by UV ozone oxidation, and masked vacuum deposition of a multilayer Al/Ti/Au (20/10/30 nm) emitter form the tunnel-junction hot-electron injector. The devices were then etched into mesas and wire bonded. Figure 2 shows a photomicrograph of a processed device after wire bonding. All the measurements were performed in an optical cryostat at 77 K to reduce hole thermionic leakage current.[5] Luminescence was collected through a pair of convex lens into a multimode optical fiber and the

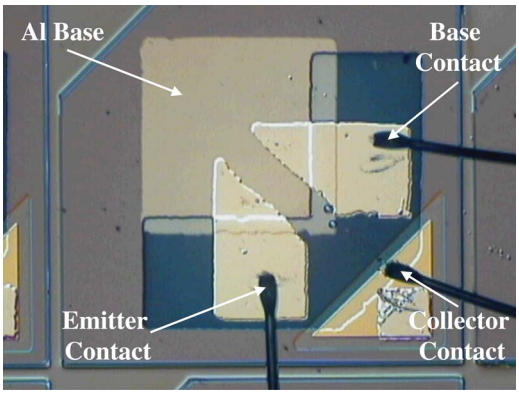

FIG. 2. (Color online) Photomicrograph of a processed vertically integrated BEEL device. Electrical contact to the collector is made by etching down to the p^+ layer (triangle area) followed by the deposition of Cr/Au lead (smaller triangle).

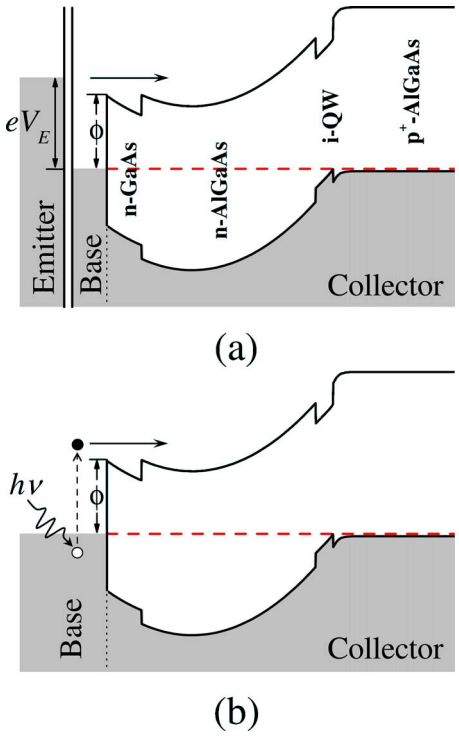

FIG. 3. (Color online) Schematic energy band diagrams of a BEEL device (a) and an IPEL device (b) with collectors unbiased. Hot electrons are injected into the semiconductor by tunnel emission (a) or internal photoemission (b) mechanisms.

spectra were recorded with a Thermo-Oriel MS257 1/4 m spectrograph with a thermoelectric-cooled Si charge coupled device (CCD) and a diffraction grating with 150 lines/mm and a blaze wavelength of 800 nm.[3]

Although lateral luminescence contrast is not expected for the relatively uniform GaAs QW active region, devices terminated with 80 Å thick Au thin-film base that forms a Schottky contact with the semiconductor surface were also fabricated for STM mode studies. The details of device processing can be found in Ref. 4. As an equivalent method to tunnel emission, internal photoemission (IPE) was used to inject hot electrons photoexcited in the Au base over the Schottky barrier into the semiconductor using a monochromatic sub-bandgap illumination (see Fig. 3). Internal photoemission luminescence (IPEL) may be induced given enough collector bias.[13] Each device was characterized by IPEL before STM measurement was performed. It is found to be an indispensable quality-filtering step for STM experiments, which typically allow only one device to be tested per operation.

IV. DEVICE CHARACTERIZATIONS

A. Performance of integrated photodetector

In Fig. 4, under the condition of ballistic injection (emitter negatively biased at −1.4 V), collector current (triangles) as a function of collector bias is presented. Collector current exhibits a "turn-on" threshold between 0.9 and 1.0 V, which is close to the observed collector current threshold near 0.8 V for the original BEEL device (Fig. 2 in Ref. 3). The slight increase of the apparent threshold may result from the

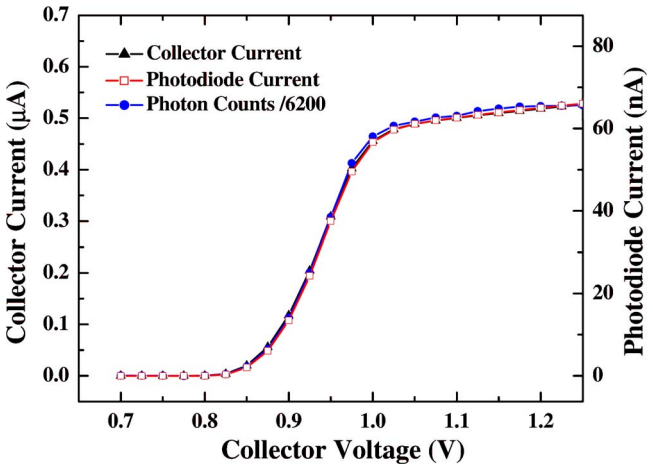

FIG. 4. (Color online) Comparison of collector bias dependence of collector current (closed triangles), on-device photodiode current (open squares), and externally collected luminescence (closed circles) at a constant emitter bias of −1.4 V at 77 K.

voltage drop across the p^+ layer because of the in-plane resistance or contact resistance in the present integrated-optics device.

In the same figure, the collector-voltage dependence of the peak magnitude of the luminescence (scaled) collected by the CCD (circles) is superimposed. The photon emission from the GaAs QW accompanies the increase in collector current at the collector bias threshold, consistent with the observed relationship between collector current and luminescence intensity in the original BEEL device.[3] Because of the required energy conservation, a collector bias in excess of the difference between the GaAs band gap and the Schottky barrier height is needed to convert the kinetic energies of hot electrons into photons.

The current across the *unbiased* GaAs/InGaAs SL photodiode, supposedly induced from interband excitations by photons emitted from the GaAs QW, is recorded simultaneously with the collector current and luminescence. It is also shown in Fig. 4 (squares). The collector-voltage dependence of this current closely mimics both the hot-electron collector current and the externally detected photon intensity, with an amplitude more than 13% of the collector current. The similarity in collector bias dependence of all three of these signals is a strong evidence that a significant fraction of emitted photons produces photoexcitation in the integrated photodiode. However, it does not completely eliminate the possibility that the photodiode current is induced from leakage of electrons through the p^+ layer, analogous to the minority current in the base of a HBT.

To rule out this possibility, further evidence is needed. There are at least two pieces of evidence that support the picture that photodiode current originates from photoexcitation rather than bipolar injection. First, the photodiode is forward biased to measure the GaAs/InGaAs SL band edge electroluminescence (EL). Shown in Fig. 5, the EL peak is clearly at a lower energy than the BEEL peak (1.484 eV vs 1.506 eV), which shows that the photodiode must be sensitive to the interband BEEL emission from the GaAs QW.

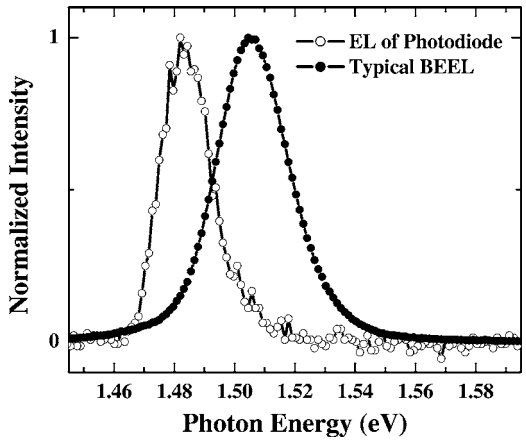

FIG. 5. Comparison of the BEEL spectrum (closed circles) with the electroluminescence of forward-biased on-device photodiode (open circles) at 77 K.

The second positive evidence is shown in Fig. 6. In addition to monitoring the three signals of collector current, luminescence intensity, and photodiode current on the same integrated-optics device, current across an *unbiased* photodiode that resides on an adjacent device on the same chip is recorded simultaneously. The adjacent photodiode is electrically isolated from the monitored device by the etched mesas, and the tunnel-junction emitter and base on that device are disconnected (the geometry of the measurement is illustrated at the top of Fig. 6). This guarantees that any measurable signal on the adjacent photodiode is induced by photoexcitation only but not electron leakage. Indeed, the adjacent photodiode detects a photocurrent that mimics the behaviors of on-device photocurrent as well as the photon intensity recorded with conventional far-field techniques, albeit the amplitude is only roughly 0.25% of the on-device photocurrent because of the much weaker optical coupling. This strongly implies that for the measured collector bias range up to ≈1.3 V, the current signal detected in the photodiode is

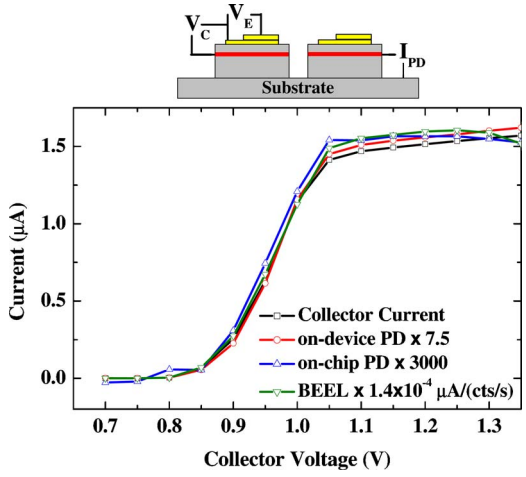

FIG. 6. (Color online) Schematic of the measurement configuration (above) and comparison of collector bias dependence of collector current (squares), on-device photodiode current (circles), adjacent photodiode current (up triangles), and externally collected luminescence (down triangles) simultaneously measured at a constant emitter bias of −1.5 V at 77 K.

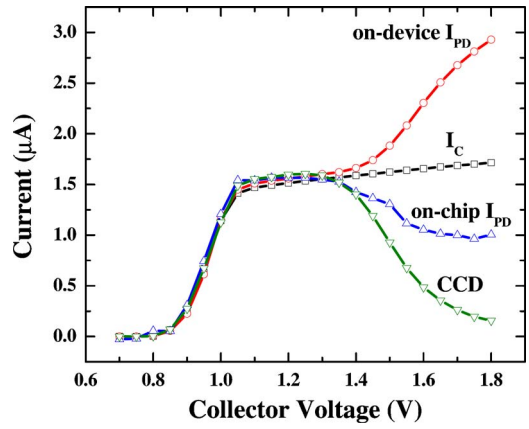

FIG. 7. (Color online) A wider range plot of Fig. 6 showing extra on-device photodiode current accompanied with drop of adjacent photodiode current and luminescence intensity at collector bias higher than 1.3 V.

only due to photoexcitation, not to minority leakage through p^+ layer.

B. Parasitic bipolar injection

However, the situation is drastically changed at a collector bias higher than ~1.3 V. In Fig. 7, the same data in Fig. 6 are replotted with a wider collector bias range. Although collector current continues to increase without any characteristic change, on-device photodiode current surges, accompanied with a drop of far-field luminescence intensity. Meanwhile, current detected in the adjacent photodiode follows the far-field luminescence signal, indicating that indeed the photon emission decreases at collector bias higher than ~1.3 V. Therefore it is suspicious that the additional current detected by the photodiode directly beneath the luminescent device is from the photoexcitation. Figures 8–10 present three-dimensional surface plots of all the three signals (collector current, photodiode current, and luminescence) measured from the same device.

Since the doping profile of the present device is somewhat similar to a HBT, it is possible that bipolar injection of minority electrons through p^+ layers happens at enough collector bias. To clarify this possibility, one needs to carry out

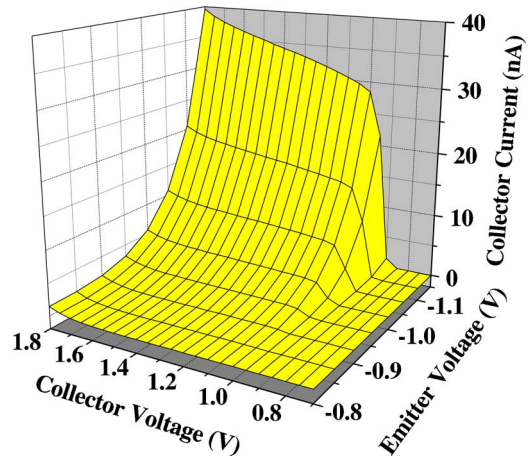

FIG. 8. (Color online) Collector current spectroscopy for an integrated-optics BEEL device at 77 K.

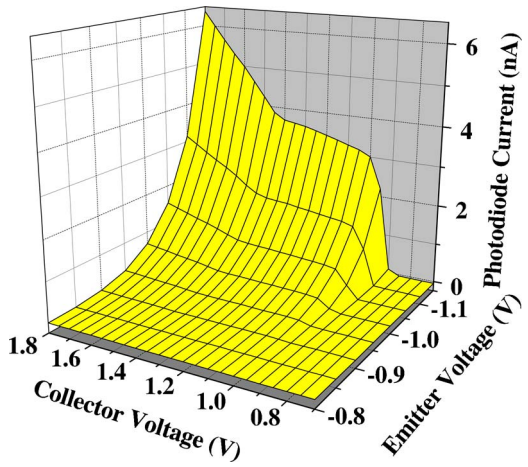

FIG. 9. (Color online) On-device photodiode current spectroscopy simultaneously measured with Fig. 8.

a more detailed characterization of the semiconductor heterostructure in a three-terminal transistor configuration. Different from the configuration of metal-base transistor for BEEL operations, where emitter and base are the two electrodes of tunnel junctions, the semiconductor heterostructure itself can be redefined as a bipolar transistor (see Fig. 1). From now on, the surface n-type region is called the "emitter," the p^+ layer is called the "base," and the n^+ substrate is called the "collector." The equivalent circuit diagrams (in a simplified version) are illustrated in Fig. 11 for both common-emitter mode and common-base mode operations.

The common-base mode operation has the same configuration as the normal BEEL operation. Hot electrons are externally injected (by tunnel emission or IPE) into the emitter as majority carriers. At high enough base-to-emitter bias V_{BE} (the same as the collector bias for BEEL), these electrons are injected as minority carriers into the space charge region (GaAs QW) where most of them are recombined with holes and emit photons. Because of the very high electron capture cross section of GaAs QW at low temperatures, very few electrons can escape into the p^+ layer beneath the QW, where bulk recombination (nonradiative) with holes and an energy barrier at the etch-stop layer further decrease the electron leakage. The present design (elongated base with heavy p doping and an $Al_{0.3}Ga_{0.7}As/Al_{0.45}Ga_{0.55}As$ heterojunction) is aimed to entirely eliminate the *direct* common-base current gain, i.e., bipolar injection of electrons into the collector, whereas maximize the *apparent* common-base current gain induced by photogeneration in the GaAs/InGaAs SL absorption layer. For the present device, the apparent common-base gain is about 0.1, which can be boosted higher than unity by using an avalanche photodetector.

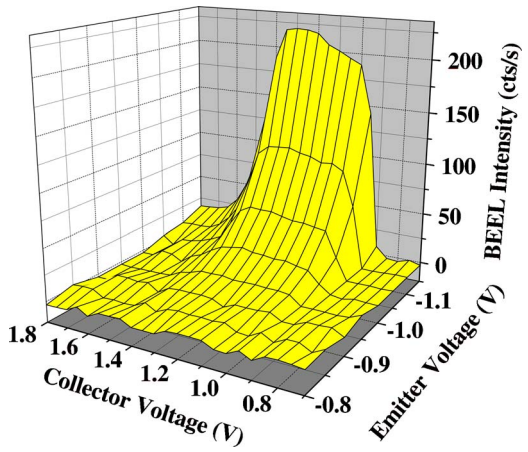

FIG. 10. (Color online) BEEL intensity spectroscopy simultaneously measured with Fig. 8.

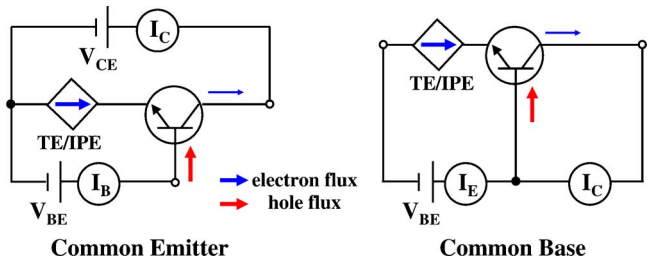

FIG. 11. (Color online) Equivalent circuit diagrams for an integrated-optics BEEL device operating in common-emitter mode (left) and common-base mode (right). TE/IPE stands for tunnel emission/internal photoemission injection of hot electrons.

Using IPE as an equivalent hot-electron injection mechanism, the common-base characteristic is first measured, as shown in Fig. 12. Photodiode current (now called collector current) mimics emitter current at $V_{BE} < 1.36$ V. If $V_{BE} > 1.36$ V, however, the slope of collector current increases while the slope of emitter current remains unaltered. As expected, the behavior is similar to the case of tunnel emission in Fig. 7. From the circuit perspective, emitter current always equals the sum of collector current and base current (see Fig. 11). An enhanced collector current should be accompanied with a corresponding decrease of base current. In common-base mode, only emitter current and collector current are measurable, whereas in common-emitter mode only base

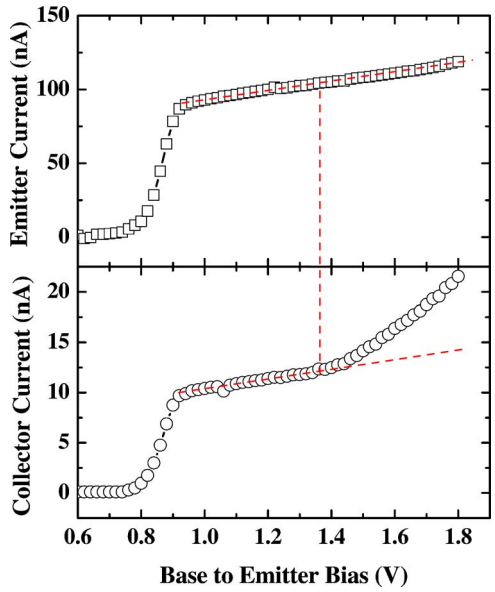

FIG. 12. (Color online) Common-base mode Gummel I-V characteristics of an integrated-optics IPEL device illuminated by a 1060 nm (1.17 eV) laser measured at 77 K. Dashed lines are to guide the eye.

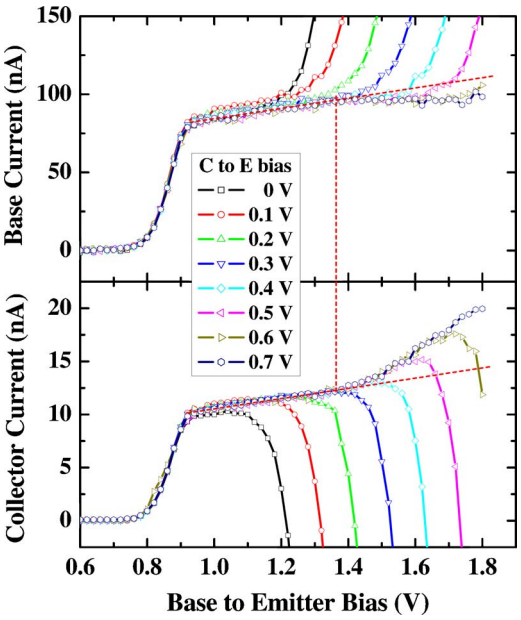

FIG. 13. (Color online) Common-emitter mode Gummel *I-V* characteristics of the same device in Fig. 12 illuminated by a 1060 nm (1.17 eV) laser measured at constant collector-to-emitter biases from 0 to 0.7 V at 77 K. Dashed lines are to guide the eye.

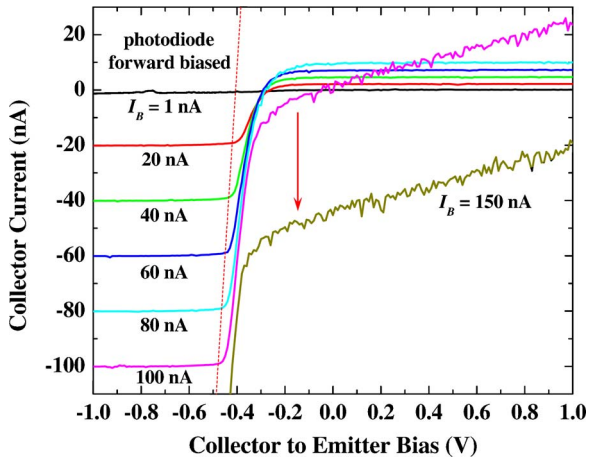

FIG. 14. (Color online) Common-emitter mode collector characteristics of the same device in Fig. 12 illuminated by a 1060 nm (1.17 eV) laser measured at constant base currents at 77 K. Notice the drastic change for base current larger than 100 nA.

current and collector current are measurable. Therefore a complementary common-emitter mode test is needed to see if this indeed happens.

In Fig. 13, common-emitter characteristics of the same device are presented. Noticeably, a positive V_{BE} is equivalently a forward bias for the *p-i-n* photodiode, which will be "turned on" at $V_{BE}>1$ V. The exponential increasing collector current and base current overwhelm the very small emitter current (limited by the hot-electron injection level) and the device behaves like a two-terminal *pn* diode. A positive collector-to-emitter bias V_{CE} is needed to keep the photodiode from being turned on.

By applying a constant positive V_{CE}, it is observed that the turn-on threshold of the photodiode is indeed shifted higher by the amount of V_{CE}. At $V_{CE}=0.7$ V, the characteristic of collector current remains BEEL-like (three-terminal operation) up to the maximum applied V_{BE} of 1.8 V, with an enhancement at $V_{BE}>1.36$ V similar to what was seen in common-base mode. The simultaneously measured base current shows a corresponding *decrease* at $V_{BE}>1.36$ V, although the current drop is not as obvious because of the much larger amplitude of base current. This implies that the additional collector current seen at $V_{BE}>1.36$ V originates from a bipolar operation: a fraction of minority electrons is injected through the p^+ layer, and therefore causing an increased photodetector current and a corresponding drop of spontaneous emission.

To further illuminate the possible HBT operations, a straightforward way to view the current gain is to measure the so-called "collector characteristics" in common-emitter mode, by sourcing a constant base current (I_B) and measuring the collector-to-emitter *I-V* characteristics. The result is plotted in Fig. 14, using the same illumination condition (1.17 eV laser) on the same device. At $V_{CE}>-0.3$ V, the device operates in *forward active* region as a bipolar transistor, with the collector current (I_C) quickly saturates at a nearly constant large-signal current gain $\beta_{dc}=I_C/I_B\sim 12\%$. For a clearer view, see Fig. 15. Notice that almost all of the current gain is from optical coupling, i.e., electron-hole recombination and photon emission in the GaAs QW and photoexcitation in GaAs/InGaAs SL, rather than electrical coupling, i.e., direct minority injection through the base. At $V_{CE}<-0.3$ V, which corresponds to *reverse active* region of a transistor, the sign of I_C is reversed and the amplitude exponentially increases to a saturation value that equals the sourced I_B at $V_{CE}\leqslant -0.4$ V, which results from the turn-on of the *p-i-n* photodiode under forward bias.

If I_B is sourced more than $\sim$100 nA, which corresponds to $V_{BE}>1.36$ V, the collector characteristics suddenly change. I_C now increases linearly with V_{CE} without showing any saturation in forward active region. Further increment of the sourced I_B does not change the shape of I_C, instead the curve is downshifted by roughly 90% of the I_B increment. The drastic change of collector characteristics at I_B

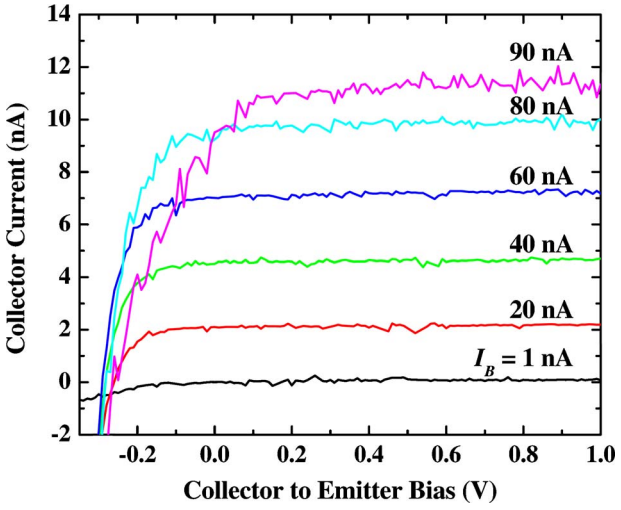

FIG. 15. (Color online) A close look at Fig. 14 showing the active region of the bipolar operation. Deviation is noticeable at a base current of 90 nA.

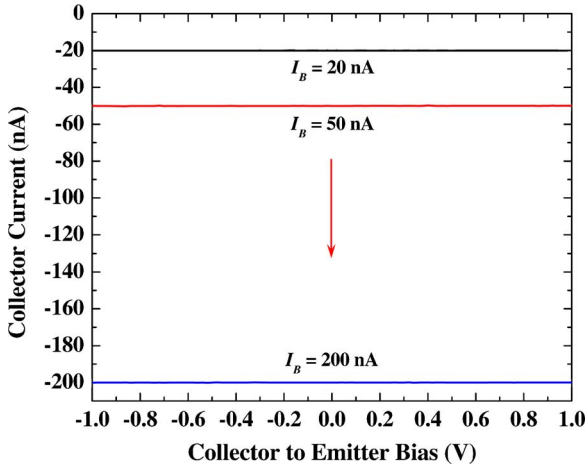

FIG. 16. (Color online) Common-emitter mode collector characteristics for the same device shown in Fig. 14 without illumination.

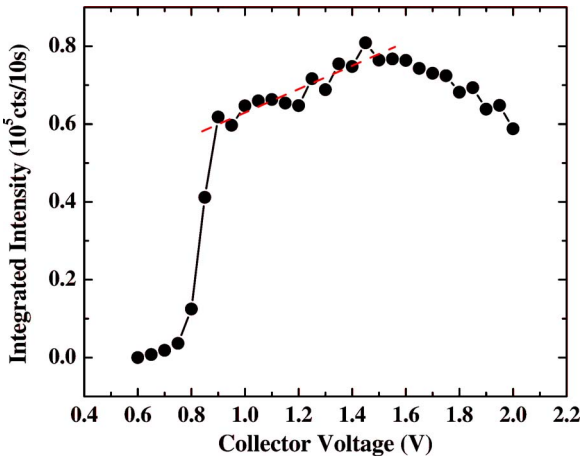

FIG. 17. (Color online) Collector bias dependence of far-field integrated luminescence intensity collected from the backside of an IPEL sample at 77 K. Dashed line is to guide the eye.

$\geqslant$100 nA with an enhanced current gain is a clear evidence that direct bipolar injection of minority electrons through the p^+ layer occurs. The downshift of I_C at even higher I_B can be explained by the hole current been "forced" into the collector, since I_B is sourced beyond the maximum hot-electron injection level.

By turning off the illumination and hence the hot-electron injection, the emitter is essentially *cut off*. The device now works just like a two-terminal *pn* diode with base and collector electrodes forming the circuit loop (see Fig. 11 left). Shown in Fig. 16, the measured collector current equals base current without showing any voltage dependence.

Although the above results are strong evidences for HBT operations, there remains other possibilities that need to be ruled out. The observed drop of front-side far-field luminescence may be originated from *redistribution* of photon emission. Since the optical length (distance times refractive index) from the active region to the surface roughly equals half of the emission wavelength ($\lambda \approx 830$ nm), the metal base may act as a partial reflector (mirror) to cause an interference effect that changes the emission pattern.[14] However, such an interference effect, if exist, should be voltage independent. Coupling to surface plasmon-polariton (SPP) modes may also reduce the front-side emission intensity, since these SPP modes are essentially nonradiative in the absence of scattering.[15] The voltage dependence is still difficult to understand. Since the possibility of either interference or SPP does not exist on the substrate side, photon emission collected from the backside may show a similar enhancement as seen in photodiode current.

As a proof, far-field luminescence is collected from the backside with simultaneous electrical measurements described above. The front side of the device (Au base) is illuminated with a 1060 nm laser to inject hot electrons. The pump line background is removed by a 900 nm short-pass filter. The collector current and photodiode current behave similar to the observations in front-side collection (the definitions used for BEEL are recovered from now on). The backside far-field luminescence (Fig. 17), however, also shows a decrease at collector bias higher than $\sim$1.4 V, which is similar to the case of front-side luminescence. Therefore it is unambiguously concluded that the accompanied enhancement of on-device photodiode current originates from parasitic bipolar injection.

Now one has to explain the reason of parasitic bipolar injection at collector bias higher than $\sim$1.3 V. Although the total thickness of the p^+ layer beneath the GaAs QW is about 300 nm, it is still much smaller than the electron minority diffusion length [$\sim 1\ \mu$m (Ref. 16)]. However, electron diffusion should be stopped by the potential barrier ($\approx$180 meV) made by the $Al_{0.45}Ga_{0.55}As$ layer, given that thermionic emission over the barrier is eliminated at low temperatures. A plausible explanation is that the finite resistivity of the thin films results in a proportional fraction of the collector bias dropped across the p^+ layer, which may null the potential barrier by the $Al_{0.45}Ga_{0.55}As$ layer and cause electron leakage. To eliminate the minority leakage current, the thickness of the p^+ layer may be increased and higher potential barrier made by heterojunction with larger band offset may be fabricated.

C. Discussion

We can now analyze the results from the standpoint of developing BEEL into a microscopy technique capable of spatially resolving the presence of luminescent layers buried beneath the metal-semiconductor interface. As discussed previously, in STM mode, a typical tunneling current of 10^0–10^1 nA will produce a collector current of 10^0–10^2 pA. With the integrated photodiode exhibiting more than 10% detection efficiency, this is expected to produce 10^{-1}–10^1 pA photocurrent, which is readily detectable by high-gain current preamplifiers. Although the gain of a *p-i-n* photodiode is at most unity, it can be replaced by an avalanche photodiode to obtain a gain much larger than 1.[17] From the instrumentation point of view, direct integration of the photodetector into the luminescent device eliminates the necessity for accommodating optical elements (fibers, lenses, etc.) into the microscope apparatus. Only modest modifications on the existing STM system are needed, including additional electrical contacts to the specimen for simultaneous collector current

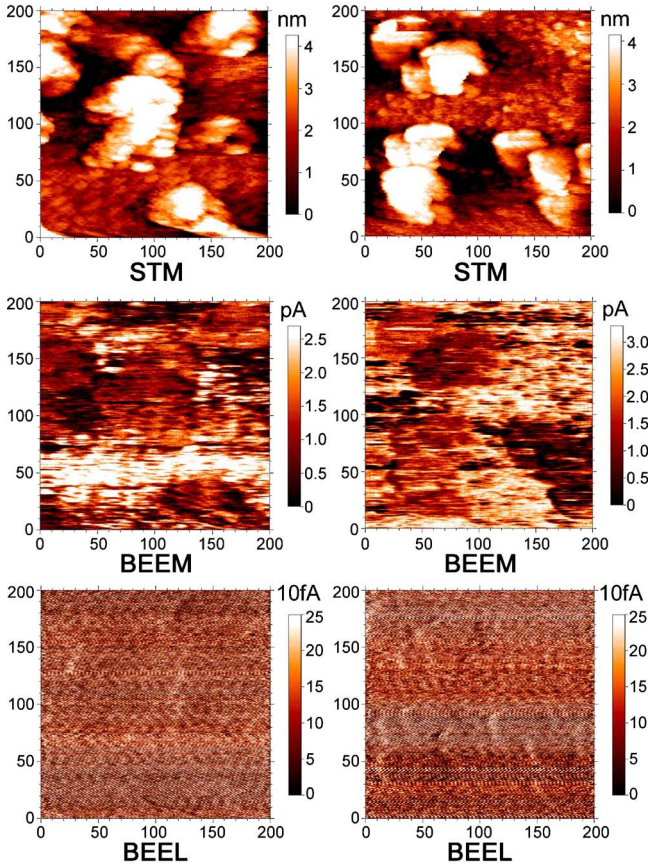

FIG. 18. (Color online) Concurrent STM (Z), BEEM (I_C), and BEEL (I_{PD}) images acquired at V_C equals 0.8 V (left) and 1.0 V (right) at 118 K. Tip bias is −1.5 V and tunnel current is 1 nA. Scanning area is 200×200 nm^2.

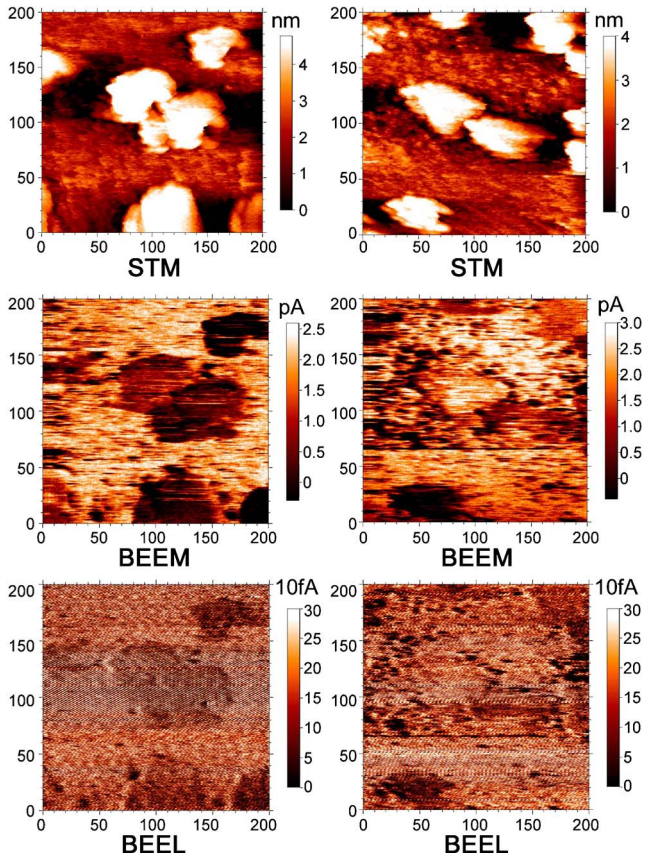

FIG. 19. (Color online) Concurrent STM (Z), BEEM (I_C), and BEEL (I_{PD}) images acquired at V_C equals 1.2 V (left) and 1.4 V (right) at 118 K. Tip bias is −1.5 V and tunnel current is 1 nA. Scanning area is 200×200 nm^2.

and photocurrent measurements, additional high-gain current amplifiers, and extra analog-to-digital (A/D) signal channels for the microscope controller.

V. BEEL MICROSCOPY

A. Experimental details

Since the integrated photodiode drastically improves the photon detection efficiency, it is interesting to test the device in microscopy mode. Devices for STM study were fabricated the same way as for IPEL study in the last section, with a thin (80 Å) Au base forming a Schottky contact to the sample surface. Hot electrons are injected by the STM tip into the base, which ballistically traverse the base over the Schottky barrier into the semiconductor collector. The measurements were performed in a variable-temperature STM system (Omicron VT-25 AFM/STM) operating under ultrahigh vacuum (UHV) conditions. Electrochemically etched Pt/Ir tips were used. The specimen holder was modified to acquire independent electrical contacts to the Au base, collector, and substrate (photodiode). Processed wafers were cut into slices to be mounted to the specimen holder and the electric contacts were made by wire bonding. Care was taken to isolate the sample from any light source to avoid the induced photocurrent. The sample was first cooled down to 100–120 K by a continuous flow of liquid nitrogen. After the temperature was stabilized, the tip approach was performed. Negative tip bias higher than Schottky barrier (≈0.8 eV) was applied to inject hot electrons. Images were acquired by scanning the tip position at a constant tip tunnel current (1 nA) and a constant positive collector bias. Concurrent STM image (topographical Z signal), BEEM image (collector current I_C), and BEEL image (photodiode current I_{PD}) were acquired by first converting I_C and I_{PD} to voltage signals using current preamplifiers with gains of 10^9 and 2×10^{10} V/A, respectively. The signals are then fed into the extra A/D channels of the STM controller.

B. Microscopy results

Figures 18 and 19 show four sets of images acquired on such an integrated device measured at increasing collector bias (V_C) from 0.8 to 1.4 V at an interval of 0.2 V. Tip bias was −1.5 V and tip tunnel current was 1 nA. The scanned area was 200×200 nm^2. Large scale STM images reveal that the surface is covered by scattered particles with typical lateral sizes of 50–100 nm and heights of 5–10 nm. These particles are much larger than grains of polycrystalline Au film (typically 5–15 nm in size and 1–2 nm in height). They are probably produced by the wafer-cutting or wire-bonding process. The presence of these particles may disrupt the tip scanning and produce fluctuations of tip tunnel current despite the feedback control. However, they provide an unintentional "modulation" of collector current injection level. Indeed, in Fig. 18, BEEM images show less collector current

(darker) in areas covered with particles (bright features in STM images). Since $V_C=0.8$ V is at around the collector current turn-on threshold (0.85 V for this device), the BEEM image is relatively dark (small signal) and the concurrent BEEL image is essentially featureless. The situation is only slightly improved at $V_C=1.0$ V. The BEEM image now clearly shows darker areas correlated with particles seen in the STM image. The contrast of BEEL image is still very weak. The subsequent images taken at $V_C=1.2$ V and $V_C=1.4$ V (Fig. 19) start to show obvious contrasts in BEEL images, which are strongly correlated with the corresponding BEEM images. Keep in mind that the present sample has a homogeneous luminescent layer (GaAs QW), it is not surprising that any modulation of collector current will produce a proportional modulation on luminescence intensity and subsequently photocurrent. Since the photon detection mechanism has been shown by the solid-state metal-base transistors, the present results strengthen the promise of BEEL as a microscopy tool for subsurface photonic imaging of semiconductor nanostructures.

VI. SUMMARY

In this article, taking advantage of epitaxial growth technique, we have tested the feasibility of directly integrating a photodetector (a *p-i-n* photodiode for the present case) into a ballistic electron emission luminescence (BEEL) heterostructure. Results from solid-state tunnel emission devices using this design concept are very promising. More than 10% of the photons emitted by the GaAs quantum well excite photoelectrons in the photodetector grown just below the luminescent layer. The close distance, the improved optical coupling with index matching, and the large effective collection angle in this scheme improve the detection efficiency of BEEL signal by many orders of magnitude as compared to any far-field detection scheme using conventional optical components. An abnormal increase of photocurrent accompanied by a drop of far-field BEEL signal is observed above a characteristic collector bias, which is shown to be from parasitic bipolar injection. This issue can be overcome by improved device design, or simply by limiting the operating range of collector bias. Finally, preliminary BEEL microscopy results using a STM tip as the ballistic electron injector are presented. By using a homogeneous luminescent layer, the observed BEEL (photocurrent) images show lateral variations correlated with simultaneously acquired BEEM (collector current) images. The latter reflect inhomogeneities of ballistic electron injection at the metal-semiconductor interface, or fluctuations of tunnel current by nonconductive impurities or abrupt surface features. In conclusion, the prospects for BEEL microscopy have been simplified and strengthened.

ACKNOWLEDGMENTS

One of the authors (W. Y.) thanks S. Tiwari for helpful discussion. This research is supported by the NSF under Grant No. ECS-0322720, the Harvard NSF-funded Nanoscale Science and Engineering Center (NSEC), and partly by an DARPA HUNT subaward (222891-01) from the University of Illinois.

[1] W. J. Kaiser and L. D. Bell, Phys. Rev. Lett. **60**, 1406 (1988).
[2] For reviews, see M. Prietsch, Phys. Rep. **253**, 163 (1995); V. Narayanamurti and M. Kozhevnikov, *ibid.* **349**, 447 (2001); J. Smoliner, D. Rakoczy, and M. Kast, Rep. Prog. Phys. **67**, 1863 (2004).
[3] I. Appelbaum *et al.*, Appl. Phys. Lett. **82**, 4498 (2003).
[4] I. Appelbaum, K. J. Russell, M. Kozhevnikov, V. Narayanamurti, M. P. Hanson, and A. C. Gossard, Appl. Phys. Lett. **84**, 547 (2004).
[5] W. Yi, I. Appelbaum, K. J. Russell, V. Narayanamurti, M. P. Hanson, and A. C. Gossard, Appl. Phys. Lett. **85**, 1990 (2004).
[6] A. Fiore, J. X. Chen, and M. Ilegems, Appl. Phys. Lett. **81**, 1756 (2002).
[7] S. Fafard, K. Hinzer, S. Raymond, M. Dion, J. McCaffrey, Y. Feng, and S. Charbonneau, Science **274**, 1350 (1996).
[8] J. C. Blakesley, P. See, A. J. Shields, B. E. Kardyna, P. Atkinson, I. Farrer, and D. A. Ritchie, Phys. Rev. Lett. **94**, 067401 (2005).
[9] B. O. Dabbousi, M. G. Bawendi, O. Onitsuka, and M. F. Rubner, Appl. Phys. Lett. **66**, 1316 (1995).
[10] W. Yi, Ph.D. thesis, Harvard University, 2005.
[11] V. Ryzhii, M. Ershov, M. Ryzhii, and I. Khmyrova, Jpn. J. Appl. Phys., Part 2 **34**, L38 (1995).
[12] H. C. Liu, J. Li, Z. R. Wasilewski, and M. Buchanan, Electron. Lett. **31**, 832 (1995).
[13] K. J. Russell, I. Appelbaum, H. Temkin, C. H. Perry, V. Narayanamurti, M. P. Hanson, and A. C. Gossard, Appl. Phys. Lett. **82**, 2960 (2003).
[14] K. H. Drexhage, J. Lumin. **1**, 693 (1970).
[15] R. R. Chance, A. Prock, and R. Silbey, Adv. Chem. Phys. **37**, 1 (1973).
[16] B. M. Keyes, D. J. Dunlavy, R. K. Ahrenkiel, S. E. Asher, L. D. Partain, D. D. Liu, and M. S. Kuryla, J. Vac. Sci. Technol. A **8**, 2004 (1990).
[17] K. J. Russell *et al.*, Appl. Phys. Lett. **85**, 4502 (2004).